Multibaseline TanDEM-X Mangrove Height Estimation: The Selection of the Vertical Wavenumber

Seung-Kuk Lee ⓘD, Temilola E. Fatoyinbo ⓘD, David Lagomasino, Emanuelle Feliciano, and Carl Trettin

Abstract—We generated a large-scale mangrove forest height map using multiple TanDEM-X (TDX) interferometric synthetic aperture radar (InSAR) acquisitions with various spatial baselines in order to improve the height estimation accuracy across a wide range of forest heights. The forest height inversion using InSAR data is strongly dependent upon the vertical wavenumber (i.e., perpendicular baseline). First, we investigated the role of the vertical wavenumber in forest height inversion from InSAR data using the sensitivity of the interferometric (volume) coherence to forest height. We used corrected but lower resolution and accuracy Shuttle Radar Topography Mission (SRTM) mangrove height maps as *a priori* information over Akanda and Pongara National Parks in Gabon to estimate lower and upper boundaries of the vertical wavenumber over test sites from the measured coherence-to-height sensitivity. Only TDX acquisitions within the boundaries of the vertical wavenumber were selected and combined for multibaseline mangrove height inversion. Mangrove forest height was obtained with multibaseline TDX acquisitions and was validated against the reference height derived from field measurement data providing improvements in multibaseline inversion over existing height estimates (i.e., SRTM height) and single-baseline inversions (multibaseline inversion: $r^2 = 0.98$, root mean square error (RMSE) of 2.73 m; SRTM height: $r^2 = 0.86$, RMSE = 7.21 m; single-baseline inversions: $r^2 = 0.08$-0.97, RMSE = 3.86–11.10 m). As a result, to accurately estimate forest heights over a wide range (3–60 m), multibaseline InSAR acquisitions (at least three different baselines) are needed to exclude biases associated with the vertical wavenumber in forest height inversion.

Index Terms—Forest height inversion, interferometric synthetic aperture radar (InSAR), multibaseline, TanDEM-X (TDX), vertical wavenumber.

I. INTRODUCTION

TOP-OF-CANOPY height information over forests is invaluable information for a wide range of mangrove forest management and conservation applications, such as illegal logging, degradation, forest declination, and growth, as well as for the allometric estimation of above-ground forest biomass [1]–[3]. Traditionally, three-dimensional (3-D) mangrove forest parameters including forest height and biomass have been quantitatively estimated by carrying out forest inventory assessments. The ground measurements in mangrove forests are generally very expensive, dangerous, time consuming, and staff intensive, especially within remote locations; thus, the available information on 3-D forest structure at regional and global scales are limited.

Remotely sensed observations of forested ecosystems have provided an alternative to field inventory surveys. In recent years, remote sensing (RS) data acquisition from airborne and spaceborne systems have rapidly increased for various forest applications, and reliable RS techniques for the retrieval of forest parameters from RS data have been successfully developed. Polarimetric SAR Interferometry (Pol-InSAR) is a powerful technique for the retrieval of 3-D forest structure parameters (e.g., top canopy height [4]–[6], biomass [3], [7], and forest tomography [8]). The coherent combination of both polarimetric and interferometric observations was the key element for an essential breakthrough in quantitative forest parameter estimation [9]. Quantitative estimation of forest parameters based on a single frequency (from *X*-band to *P*-band), fully polarimetric, and single-baseline configuration has been successfully carried out. Recent airborne and satellite systems have also demonstrated the potential of Pol-InSAR techniques at *P*-, *L*-, and *X*-band wavelengths to estimate, with a high accuracy, key forest parameters, such as forest height over a variety of natural and commercial forest types and terrain conditions [9]–[14].

Recently, single-baseline TanDEM-X (TDX) inversion approaches for forest height estimates have been evaluated and assessed. Dual-pol TDX datasets acquired by the TDX experimental mode have provided vegetation height estimates by means of model-based inversion of Pol-InSAR data [22]–[24]. In case of single-pol TDX acquisition, using airborne Lidar digital terrain model (DTM), several models have been proposed for forest height and biomass estimates [15]–[18], [22]. In [23], without airborne Lidar DTM data, the single polarization interferometric SAR (single-pol InSAR) inversion from TDX InSAR data at HH first provided a mangrove height map and indicated the potential for generating global-scale mangrove height and biomass maps at 12-m resolution.

The key observable thing used in InSAR and Pol-InSAR applications is the complex interferometric coherence, which includes both the interferometric correlation coefficient and the interferometric phase at polarization. The interferometric complex coherence depends on the instrument and acquisition parameters as well as on dielectric and structural parameter estimates of scatterers. It can be further decomposed into volume decorrelation related to forest parameters and nonvolumetric decorrelation contributions that cause height errors in forest height inversion [19], [20]. Among these nonvolumetric decorrelations, temporal decorrelation is the most critical factor for successful (Pol-)InSAR inversion performance in conventional repeat-pass spaceborne systems (i.e., temporal baseline: day $\sim$ weeks) [10]–[12]. Therefore, a forest height inversion from (Pol-)InSAR data has been limited to airborne SAR data at L-band and P-band, acquired with a short temporal baseline (<hours).

In addition to nonvolumetric decorrelation contributions, the interferometric vertical wavenumber of κ_z (related to the perpendicular baseline) is a key parameter for successful (Pol-)InSAR inversion [25], [26]. The vertical wavenumber of κ_z scales the height sensitivity for model-based inversions and determines the available height range possible to invert ($h_{\max} = 2\pi/\kappa_z$). Therefore, an inappropriate vertical wavenumber (e.g., too large κ_z or too small κ_z) for a certain forest height leads to problematic height inversion, resulting in the underestimation or overestimation of forest height. In [26], the role of the wavenumber κ_z on the (Pol-)InSAR inversion performance for estimating forest parameters has been addressed. A single-baseline inversion is allowed for an accurate inversion for a limited range of forest heights. In other words, multibaseline (Pol-)InSAR inversions with various vertical wavenumber are required to retrieve an accurate forest height map for a wide range of forest heights (up to $\sim$60 m) [25]–[27]. Although the impact of the vertical wavenumber on the performance of forest height estimation has been investigated and assessed [26], [28], the method of correctly selecting a good single-baseline acquisition(s) among multiple baselines without *a priori* knowledge of forest height remained uncertain. We propose an approach to achieve an accurate, large-scale forest height estimation of mangroves from multibaseline TDX InSAR acquisitions at a 12-m resolution using *a priori* information on height (e.g., previous SRTM mangrove heights [31]–[34]) by means of the κ_z ranges defined by the sensitivity of interferometric (volume) coherence to forest height. This paper shows how to effectively combine multiple TDX acquisitions to generate a mangrove height map with improved vertical height accuracy by selecting reliable baseline(s). In Section II, the single-pol approach for mangrove height estimates is reviewed and the κ_z ranges (lower and upper boundaries of κ_z) for forest height inversion are simulated using the coherence-to-height sensitivity along baselines (i.e., κ_z). Section III describes multibaseline TDX data and test sites where some of the tallest mangrove forests in the world exist. In Section IV, single-baseline and multibaseline TDX inversions are addressed and validated against field measurement data. Finally, the discussion and conclusion are presented in Section V.

II. FOREST HEIGHT INVERSION APPROACHES

A. Single-Baseline Inversion: Random Volume over Ground (RVoG) Model

The RVoG model is a widely and successfully used inversion model for forest height estimates using fully polarimetric and interferometric SAR data. A realistic scattering mechanism scenario in forests has to simultaneously consider both volume and ground layer interactions with radar signals. In the RVoG model, the two layers (volume and ground) are coherently modeled as a volume layer of a certain thickness h_V containing randomly oriented particles characterized by a scattering amplitude per unit volume $\tilde{m}_V$ and a ground layer of scatterers at $z = z_0$ with scattering amplitude m_G. The vertical distribution of (effective) scatterers $F(z)$ in the RVoG model can be described as [6], [28], [29]

$$F(z) = \tilde{m}_V e^{\frac{2\sigma}{\cos\theta_0}z} + m_G e^{\frac{2\sigma}{\cos\theta_0}h_V}\delta(z - z_0) \qquad (1)$$

where z is the vertical position and $\delta(\cdot)$ is a Dirac delta function for the vertical structure function of surface scattering. θ_0 is incidence angle and σ represents a mean extinction, expressing the sum of scattering and absorption. The interferometric complex coherence in forests is directly related to the vertical reflectivity function $F(z)$ by a normalized Fourier transformation relationship [6], [9]

$$\tilde{\gamma}(\vec{w}) = \frac{\int_0^{h_v} F(z')e^{i\kappa_z z'}dz'}{\int_0^{h_v} F(z')dz'} = e^{i\phi_0}\frac{\tilde{\gamma}_V + \mu(\vec{w})}{1 + \mu(\vec{w})} \qquad (2)$$

with

$$\tilde{\gamma}_V(h_V,\sigma;\kappa_z,\theta_0) = \frac{\int_0^{h_V} e^{\frac{2\sigma}{\cos\theta_0}z'}e^{i\kappa_z z'}dz'}{\int_0^{h_V} e^{\frac{2\sigma}{\cos\theta_0}z'}dz'} \qquad (3)$$

where $\tilde{\gamma}_V$ denotes the complex coherence for the random volume in the RVoG model. $\phi_0(=\kappa_z z_0)$ is the phase related to the ground topography z_0 in forests and $\mu(\vec{w})$ is the effective ground-to-volume amplitude ratio at a polarization $\vec{w}$. Accordingly, the interferometric coherence $\tilde{\gamma}(\vec{w})$ of (2) becomes a polarization-dependent function, depending on the ground-to-volume ratio $\mu(\vec{w})$. The vertical interferometric wavenumber κ_z scales the interferometric phase to height ratio and determines the available height range of the volume layer possible to estimate in the RVoG model. It is a function of wavelength λ, the angle difference between master and slave ranges $\Delta\theta$, and the incidence angle θ_0, described as [6], [9], [26]

$$\kappa_z = m\frac{2\pi}{\lambda}\frac{\Delta\theta}{\sin\theta_0} \qquad (4)$$

where m is the factor for interferometric acquisition mode: $m = 2$ for the monostatic case and $m = 1$ for the bistatic case (e.g., TDX single-pass interferometric mode). The maximum height possible to estimate with certain interferometric acquisition geometry is defined as $h_{\max} = 2\pi/\kappa_z$. As shown in (2) and (3), a complex interferometric coherence can be represented by the following four real forest parameters: h_V, σ, ϕ_0, and μ. With fully polarimetric interferometric data acquired in the monostatic mode, three independent complex coherences are

This article has been accepted for inclusion in a future issue of this journal. Content is final as presented, with the exception of pagination.

LEE *et al.*: MULTIBASELINE TANDEM-X MANGROVE HEIGHT ESTIMATION: THE SELECTION OF THE VERTICAL WAVENUMBER 3

available to measure six unknown parameters (h_V, σ, ϕ_0, and $\mu_{1,2,3}$) because μ is the only parameter related to polarization $\vec{w}$. Assuming no response from the ground in one polarization (e.g., $\mu_3 = 0$), (2) can be inverted into the five forest parameters (h_V, σ, ϕ_0, and $\mu_{1,2}$) with the measured three complex coherences [9]. However, in case of single-pol acquisition (i.e., only one available complex coherence), the inversion is underdetermined for forest height inversion by means of the RVoG model [9], [22], [23]. Even with the assumption of no ground contribution in the single-pol coherence ($\mu = 0$), the single-pol inversion is unbalanced with the three unknowns (h_V, σ, and ϕ_0) in the RVoG model and the single-pol complex coherence $\tilde{\gamma}(\vec{w})$. Single-pol inversion approaches were performed using single-pass InSAR data at *X*-band with airborne Lidar DTM used to estimate the ground phase [9], [15], [16], [18], [21], [22]. Recently, top canopy height of mangroves has been estimated from TDX data at HH-polarization without any external information of underlying topography [23]. Our approach also suggests estimating water level (i.e., ground phase ϕ_0 in the RVoG model) directly from TDX data using the assumption of flat topography under a mangrove forest. Through this approach, it has become possible to estimate mangrove height from single-pol TDX data using the RVoG model.

B. Multibaseline Inversion: The Selection of κ_z

The quality of the single-baseline forest height inversion by means of the RVoG model depends strongly on both the volume coherence calibration and the selection of the optimal κ_z value for a given forest height [25], [26]. In case of the single-pass TDX acquisition (i.e., no temporal decorrelation), nonvolumetric decorrelations (e.g., range/azimuth decorrelation, signal-to-noise ratio (SNR) decorrelation, etc.) can be negligible after accurately calibrating and filtering the complex interferometric coherence [19], [20], [30].

The volume decorrelation in (3) is the decorrelation of the random volume caused by different projections of the vertical component of the scatterer in two SAR images. Fig. 1(a)–(c) shows the volume coherences simulated by (3), as a function of κ_z (0.00–0.50 rad/m) with five different levels of height from 10 to 60 m and three different extinction levels of 0.00, 0.05, and 0.30 dB/m. The simulated volume coherences are calculated up to the maximum value of κ_z ($= 2\pi/h_V$) using the maximum height relation given in Section II-A. As shown in (3), volume decorrelation is directly related to the vertical distribution of (effective) scatterers $F(z)$ that is the exponential function expressed by extinction in the RVoG model. Furthermore, κ_z scales the coherence of the random volume to forest height, so that an inappropriate vertical wavenumber for a forest height leads to an ill-conditioned inversion problem. For very large κ_z values, the sensitivity of the coherence to forest height saturates at a given forest height and the inversion underestimates tall forests. On the other hand, for very small κ_z values, small residual nonvolumetric decorrelations cause large height errors especially for short forests [26]. In order to investigate the sensitivity of the random volume coherence $\tilde{\gamma}_V$ in (3) against
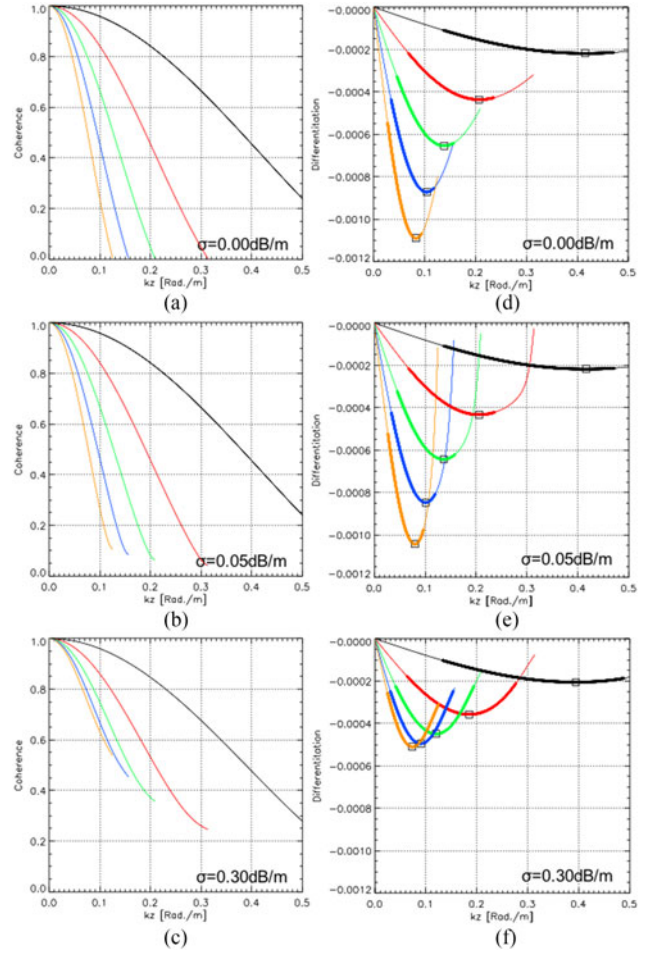

Fig. 1. Left: The amplitude of volume coherence $\tilde{\gamma}_V$ in the RVoG model as a function of the vertical wavenumber κ_z from 0.0 to 0.5 rad/m, for five different forest heights: 10 m (black), 20 m (red), 30 m (green), 40 m (blue), and 50 m (yellow) and for three different extinction values: (a) 0.00 dB/m, (b) 0.05 dB/m, (c) and 0.30 dB/m. Right: The sensitivity of the interferometric (volume) coherence γ_V to forest height as a function of κ_z, for five different heights and three extinctions. Squares represent the maximum sensitivity of the coherence to height and solid lines show the κ_z range for a good inversion performance for each forest height.

κ_z, the derivative of volume coherence f' is calculated as

$$f' = \frac{d}{d\kappa_z}\gamma_V(h_V, \sigma; \kappa_z). \tag{5}$$

The plots in the right column of Fig. 1 express that the sensitivity of the coherence to forest height with forest parameters (i.e., h_V and σ) is against κ_z. The sensitivity of the coherence to height is maximized at the minimal value of f' at each height, indicated by a square on the plots. The vertical wavenumber κ_z at the minimal value of f' (i.e., κ_z for the maximum coherence-to-height sensitivity) decreases sharply with an increase in forest height. In the case of 0.00 dB/m [see Fig. 1(d)], the coherence-to-height sensitivity for a forest height of 10 m becomes the maximum at a vertical wavenumber of 0.415 rad/m, while for a height of 50 m, much smaller κ_z of 0.083 rad/m should be selected for a stable inversion. The simulation results indicate
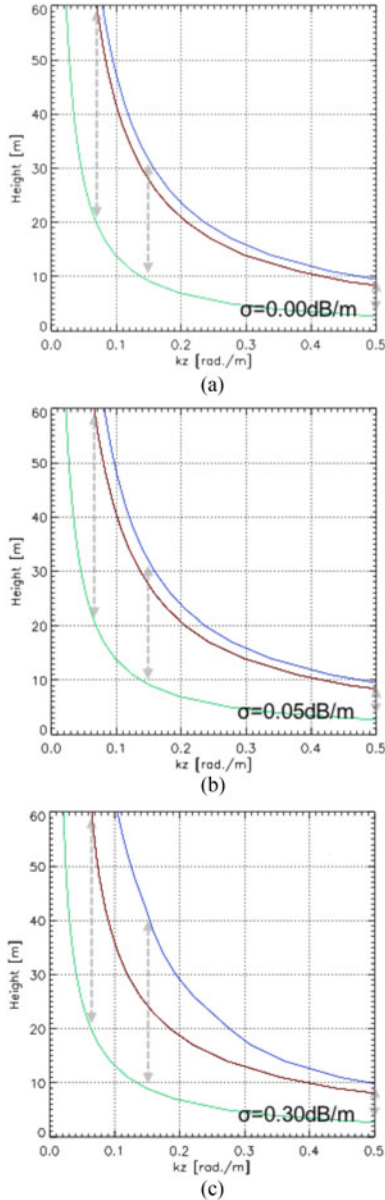
Fig. 2. Forest height inversion as a function of vertical wavenumber κ_z for three different extinctions (0.00, 0.05, and 0.30 dB/m) assuming 50% of the maximum sensitivity from volume coherence differentiation and coherence values higher than 0.3. Red: optimum curve of κ_z, green: lower boundary, and blue: upper boundary at a height range from 3 to 60 m.

that the forest height inversion depends on the choice of suitable vertical wavenumber κ_z for a given forest height.

In order to find an optimized κ_z range for a certain forest height, the vertical wavenumber at the minimal value of f' was calculated by a height range from 0 to 60 m and a vertical wavenumber from 0.00 to 0.50 rad/m. Red curves in Fig. 2 show the vertical wavenumbers for the maximum sensitivity of the coherence to height for three different levels of σ with a height range from 0 to 60 m. In other words, it is the optimal vertical wavenumber value for each forest height. As shown in the right column of Fig. 1, with an increase of κ_z, the sensitivity of the coherence to height starts to increase and becomes the maximum when f' has the minimal value (displayed by squares

on the plots). Then, the sensitivity decreases and saturates until the maximum value of κ_z ($= 2\pi/h_V$).

In this study, a κ_z range within 50% of the maximum sensitivity (i.e., the minimal value of f') is used to define upper and lower boundaries of κ_z for a reliable height inversion. Coherence values lower than 0.3 are masked out because such low coherences result in a large variance in phase and reduces the quality of height estimation [19], [26], [35]. The κ_z range defined by the threshold of the sensitivity and the coherence value is displayed by a solid line for each plot in the right column of Fig. 1. Blue and green curves in Fig. 2 express the optimized κ_z upper and lower ranges for the forest height inversion. The results indicate that for taller forests, the choice of an appropriate vertical wavenumber is restricted by the smaller range of κ_z. For example, in order to estimate a forest height of 60 m, one of multibaseline acquisitions should be located at a κ_z range between 0.023 and 0.078 rad/m [see Fig. 2(a)]. But, for the shorter forest height of 10 m, the inversion can only be accurately performed if a baseline is available at much wider κ_z range between 0.138 and 0.476 rad/m.

III. TDX DATA AND FOREST SITES

The TDX (TerraSAR-X add-on for digital elevation measurements; TDX) mission consists of two *X*-band SAR satellites, respectively, launched in 2006 and 2010 [36]. The TDX satellites have been operating in an innovative formation flying. In bistatic mode, one satellite acts as transmitter and both satellites simultaneously receive the signal backscattered by the earth's surface. This made it possible to generate a consistent global digital elevation model (DEM) with 12-m spatial resolution and unprecedented accuracy ($<$2 m) [30], [36]. To evaluate multibaseline TDX inversion of mangrove forests, a total of 31 TDX images were selected over Akanda and Pongara National Parks in Gabon (see Fig. 3). All TDX acquisitions were collected in bistatic stripmap mode (i.e., negligible temporal decorrelation effect) with single polarization of HH from January 2011 to September 2016. The interferometric vertical wavenumber of the TDX data varied from 0.057 to 0.827 rad/m (maximum height: 7.6–109.8 m). The TDX datasets consist of four levels of the vertical wavenumber (maximum height of $\sim$100 m, $\sim$80 m, $\sim$50 m, and $\sim$10 m). The TDX data for the study are summarized in Table I. Fig. 4(a) shows total number of available TDX baselines over the test sites. Most of test sites are covered by multiple TDX acquisitions with different levels of κ_z.

Forests cover 85% of Gabon and the total mangrove extent in Gabon is estimated to be 1606 km^2 [37]. Mangrove forests in Gabon are found in all estuaries, bays, and lagoons along the coast. The total area of mangrove forests within two parks was 626 km^2. In both parks, the mangroves are low-lying forests that grow around sea level and are primarily comprised of *Rhizophora* species. Tall ($>$35 m) *Rhizophora* are only found in narrow stands along the rivers. The eastern mangroves of Pongara, which grow in brackish water with a lot of sediment, are much taller and tower up to 60 m—some of the tallest mangroves in the world [37].

This article has been accepted for inclusion in a future issue of this journal. Content is final as presented, with the exception of pagination.

LEE *et al.*: MULTIBASELINE TANDEM-X MANGROVE HEIGHT ESTIMATION: THE SELECTION OF THE VERTICAL WAVENUMBER 5
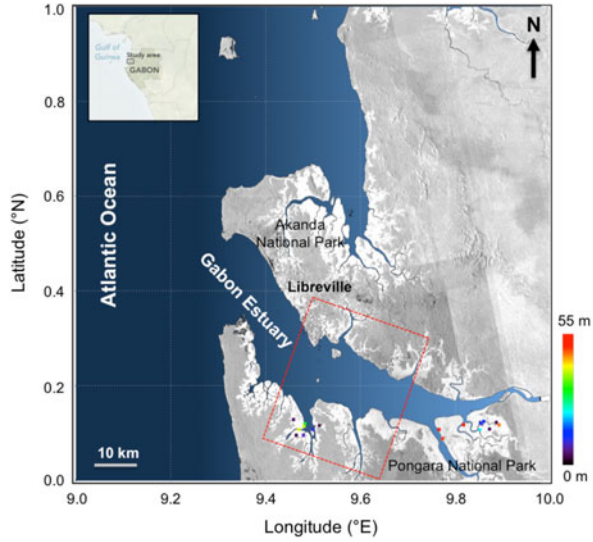

Fig. 3. Mangrove test site: Pongara National Park and Akanda National Park in Gabon. The southwestern coordinate of the image is 0.0°N latitude and 9.0 °E longitude. The frame size is 1.0° × 1.0°. The red rectangle shows a frame of a single-baseline TanDEM-X image shown in Fig. 5. Dots in the Pongara National Park represent the H100 mangrove height from field measurement data, scaled from 0 to 55 m. The grayscale base image is a TanDEM-X intensity mosaic.

TABLE I
TANDEM-X DATASETS

Date	$\left|K_z\right|$	Max Height [m]	Inc. Angle [°]	Acquisition Mode	Nr. of Scene
2011/01/19	0.142	44.1	47.7	Ascending	2
2011/03/15	0.143	44.1	46.2	Ascending	1
2011/04/28	0.117	53.7	44.5	Ascending	1
2012/11/09	0.131	47.8	46.6	Ascending	2
2013/07/15	0.123	51.1	29.8	Ascending	2
2015/09/09	0.827	7.6	46.0	Ascending	2
2015/09/20	0.578	10.9	46.1	Ascending	2
2015/10/09	0.057	109.8	46.2	Descending	2
2015/10/23	0.078	80.7	46.2	Ascending	2
2015/10/31	0.062	101.8	44.5	Descending	2
2015/11/03	0.082	76.5	44.5	Ascending	2
2015/11/09	0.170	36.9	29.8	Ascending	1
2015/11/11	0.063	100.2	47.7	Descending	2
2015/11/14	0.077	81.9	47.7	Ascending	2
2015/11/22	0.079	79.4	42.2	Descending	2
2015/12/28	0.084	74.5	46.2	Ascending	2
2016/09/01	0.784	8.0	29.8	Ascending	1
2016/09/08	0.708	8.9	29.8	Descending	1
Total					31

A frame of TDX image is ∼25 km × ∼50 km in range and azimuth. The TDX data were acquired in Stripmap imaging mode and bistatic InSAR mode. The polarization of all TDX data was HH-polarization.
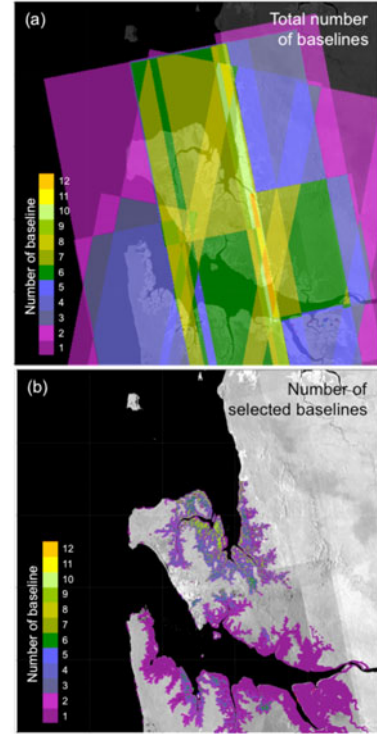

Fig. 4. (a) Total number of TDX images over Akanda and Pongara National Parks. (b) Number of selected baselines by upper and lower ranges of the vertical wavenumber for forest height estimate.

The field measurements were carried out in February 2017 to quantify mangrove carbon stocks in intact mangroves of Gabon and provided spatially-explicit field measurements of land cover, forest structure, composition, and biomass pools. Mangrove forest height derived from both SRTM and TDX data provided a basis for stratifying the field-based inventory area. A total of 18 plots (plot radius: 6.0–12.6 m) were measured and the mangrove forest within the selected inventory area represented the full range of canopy heights from 3 to 60 m. For each inventory area, individual tree height, diameter at breast height, species, and soil sediment carbon (<2 m) were measured. To compare with the inversion results, the H100 field measurement was calculated. H100 is defined as the mean height of the 100 tallest trees per hectare. It is a forestry standard canopy top height measure and corresponds to radar forest height estimates [9], [10] and airborne Lidar measurement [43].

IV. MULTIBASELINE INVERSION RESULTS FOR MANGROVE HEIGHT ESTIMATION

A. Single-Baseline Single-Pol TDX Inversion

We began SAR and InSAR processing using the coregistered single-look slant-range complex format provided by the German Aerospace Center (DLR) [38]. We measured interferometric complex coherence with ∼20 looks for fixing the postspacing of 12 m. The most advantageous result of SAR processing over mangrove forests is the much stronger backscattering power and higher amplitude of the interferometric coherence, which is often detected at the water–forest boundary [23]. The scattering
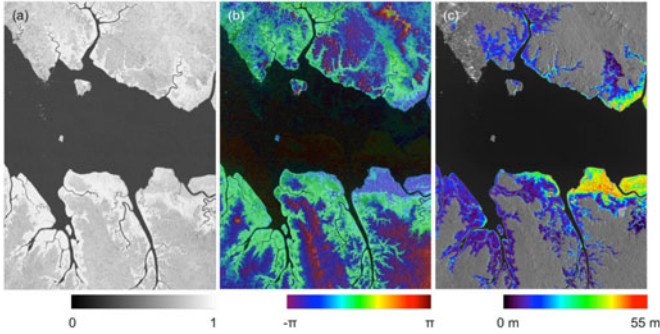
Fig. 5.   TanDEM-X images for Pongara National Park. The location of the image over the test site is displayed by the red box of Fig. 3. The TDX image was acquired on October 9, 2015. The vertical wavenumber κ_z was -0.057 rad/m. (a) Volume coherence after compensating/filtering nonvolumetric decorrelation contributions. (b) Volume only phase after eliminating the ground phase by means of water surface estimate. (c) TDX mangrove top canopy height, scaled from 0 to 55 m. The single-baseline inversion result was overlaid on the TDX amplitude image (gray).
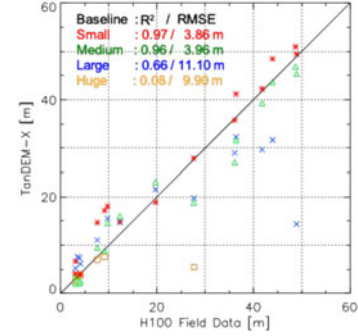

Fig. 6.   Validation plot for single-baseline TDX inversions at four different levels of κ_z (red: 0.057/0.062 rad/m, green: 0.077/0.077 rad/m, blue: 0.112/0.142 rad/m, and yellow: 0.708/0.578 rad/m) against the H100. The small baseline (red) tends to overestimation especially at small forest. In case of large baselines (blue and yellow), the sensitivity of the coherence to forest height saturates at high forests, so that the height result is underestimated.

mechanism of the radar signal at the boundary of a mangrove and water body is often detected as the double-bounce scattering. The travel path of double-bounce scattering between a mangrove tree and the open water surface on the TDX interferogram represents the elevation of the underlying topography in mangrove forests (i.e., water surface). Interferometric phases for the forest–water boundary pixels with the double-bounce dominant scattering enable us to estimate the underlying topography ϕ_0 for all mangrove forests in the image, with an assumption of flat topography in mangroves [23]. Using the TDX image, the boundaries between the mangroves and water, including open areas, lagoons, rivers, and streams, were systematically extracted by the SNR [30], [40] and the resulting double-bounce dominant targets were selected by the coherent scatterer technique [39]. Following the subtraction of the estimated ground (water) phase from the interferometric phase, the resultant volume-only phase (i.e., $\arg\{\tilde{\gamma}_V\}$) indicates the height of the interferometric phase above the ground layer. After compensating and filtering nonvolumetric decorrelations (e.g., system-induced decorrelation [30], [40] and azimuth/range decorrelations [19], [20]) that cause height errors in the forest height inversion, the coherence for random volume $\tilde{\gamma}_V$ in (3) was obtained and inverted to forest heights. Fig. 5(a) and (b) shows the volume-only coherence of TDX data acquired on October 9, 2015 and the volume phase after eliminating the ground phase. The location of TDX images is shown in the red rectangle of Fig. 3. The single-baseline TDX mangrove height estimate, scaled from 0 to 55 m is shown in Fig. 5(c). Note that for the vertical wavenumber κ_z of 0.057 rad/m, the single-pol inversion result became optimized only for forest heights taller than $\sim$20 m [see Fig. 2(b)]. In order to cover the height range smaller than 20 m, additional acquisitions with larger baseline are requested.

Fig. 6 shows the validation plot for single-baseline inversions at four different levels of κ_z [small baseline (red): 0.057/ 0.062 rad/m, medium baseline (green): 0.077/0.077 rad/m, large baseline (blue): 0.112/0.142 rad/m, and huge baseline (yellow): 0.708/0.578 rad/m] against the H100 metric. Although the inversion result at small κ_z (red) indicates a correlation coefficient

r^2 of 0.97 and an RMSE of 3.86 m for a height range from 3 to 50 m, even small residual decorrelations introduce large height errors (i.e., overestimation) at small forest heights due to the unfavorable coherence to height scaling. In the case of large κ_z values (blue), the sensitivity of the coherence to forest height saturates at forests higher than $\sim$30 m, so that the tall trees (close to the maximum height) are significantly underestimated. The inversion result at huge baseline (yellow) provides an accurate estimate only for small forests ($<$10 m), but most of the tall forests are masked out due to low coherence values ($<$0.3).

B. Multibaseline Single-Pol TDX Inversion

In order to effectively combine single-baseline inversion results with various baselines, the inversion results were first geocoded into latitude and longitude at 12-m resolution. The baselines between the lower and upper boundaries in Fig. 2 were selected by using *a priori* knowledge of height. For initial height information, the mangrove height map was used, which was derived from the SRTM and Ice, Cloud, and Land Elevation Satellite/Geoscience Laser Altimeter System generated from a previous study [33] [see Fig. 7(a)]; although those systems had relatively low spatial resolution and accuracy. Lower and upper boundaries of vertical wavenumber over the test site were defined using the forest height of SRTM (adding uncertainty of $\pm$10%) and the coherence threshold of 0.3 by means of the simulation in Section II-B [see Fig. 7(c) and (d)]. The results show that for a given height, there is only a certain κ_z range, where a good height inversion performance is achieved. For the taller forest, the wider range of κ_z was estimated. The unfavorable single-pol height inversions that had too small κ_z or too large κ_z values were excluded. We finally measured an average of the selected single-baseline inversion results within the κ_z range, as shown in Fig. 7(c) and (d). If there is no available TDX acquisition, we chose a single-baseline inversion result with the closest baseline from the optimum κ_z, as shown in Fig. 7(b). Note that a fixed κ_z range mask (e.g., $\kappa_z < 0.05$ and $\kappa_z > 0.15$) for single-baseline acquisition suggested in [9], [10], and [26] was not necessary for this study. Fig. 4(b) shows the number of available baselines selected by the κ_z range. The
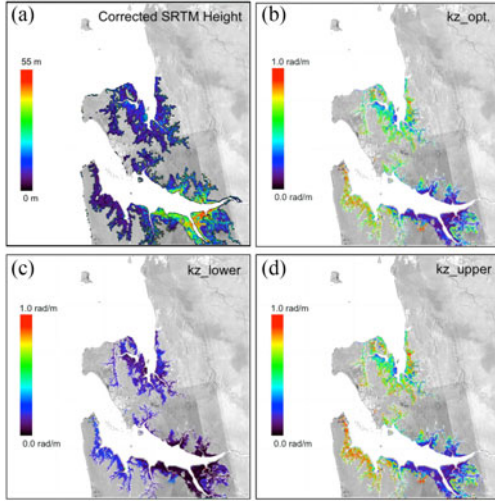
This article has been accepted for inclusion in a future issue of this journal. Content is final as presented, with the exception of pagination.

LEE *et al.*: MULTIBASELINE TANDEM-X MANGROVE HEIGHT ESTIMATION: THE SELECTION OF THE VERTICAL WAVENUMBER 7

Fig. 7. (a) Mangrove forest height from SRTM data, scaled from 0 to 55 m. (b) Optimum κ_z range over the test site from the red curve in Fig. 2(b) by means of the forest height of (a). It is scaled from 0.0 to 1.0 rad/m. (c) Lower boundary of κ_z by means of the green curve in Fig. 2(b). (d) Upper boundary of κ_z by means of the red curve in Fig. 2(b).
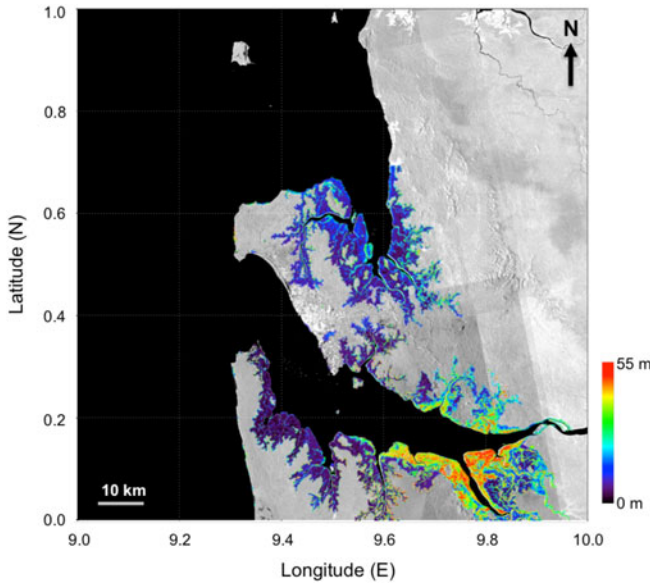

Fig. 8. Multibaseline inversion results of TDX over Pongara National Park and Akanda National Park in Gabon, scaled 0 to 55 m. Red represents areas where mangrove trees are tall. The reds appear in the Pongara National Park, where mangrove trees tower up to ~60 m.

multibaseline mangrove height map was obtained only from the selected baselines that exhibited a good sensitivity of interferometric coherence to forest height and was subsequently superimposed on the TDX amplitude image, as shown in Fig. 8. While the taller mangroves (>40 m) are further inland, the shorter mangroves (<10 m) occur closer to the mouth of the Gabon estuary as a result of higher water salinity. In Akanda National Park, the mangroves are intermediate in height, reaching up to ~20 m.

The validation plot for the Pongara mangrove forests against field H100 height is shown in Fig. 9. The result showed a good multibaseline inversion performance indicating a
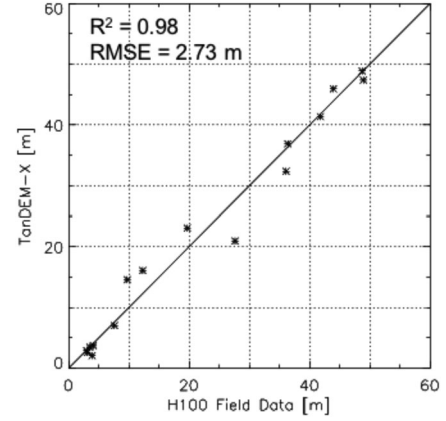

Fig. 9. Multibaseline inversion results were well correlated with the H100 from field measurement data. The range of forest height from the H100 was from 3 to 50 m. The multibaseline approach improved significantly forest height inversion performance: The correlation coefficient was 0.98 and an RMSE was 2.73 m (cf. SRTM mangrove height (see Fig. 7(a): 0.86 and an RMSE of 7.21 m and single-baseline inversions: 0.08–0.97 and RMSEs of 3.86–9.90 m).

correlation coefficient r^2 of 0.98 and an RMSE of 2.73 m, whereas the comparison of the SRTM initial height and the field H100 metric was characterized by r^2 of 0.86 and an RMSE of 7.21 m. The multibaseline inversion result also showed a substantial improvement of height estimate from 3 to 50 m, compared to the single-baseline inversions shown in Fig. 6. In case of the multibaseline inversion, there is no saturation of the sensitivity of the coherence to forest height. The estimation accuracy for the Pongara mangrove forests with a wide range of top canopy height was better than 10% for the proposed multibaseline inversion approach.

V. DISCUSSION AND CONCLUSION

Top-of-forest canopy height for mangroves was estimated from TDX HH data by means of a single-pol InSAR approach. Although the single-pol inversion approach from single-baseline TDX data has shown the potential for estimating top canopy height of mangroves, the inversion performance depends strongly on the selection of the vertical wavenumber. Single-baseline inversion results have demonstrated an unstable correlation coefficient (r^2: 0.08–0.97) and variable RMSE (3.86–9.90 m), depending on the choice of the vertical wavenumber. None of the single baseline results could provide a good forest height estimate for the entire height range between 3 and 50 m.

We investigated the influence of an optimized range of vertical wavenumber on the performance of forest height estimation. The proposed simple simulation showed the sensitivity of interferometric (volume) coherence to forest height along spatial baselines. The optimum κ_z of height inversion was detected at the maximum sensitivity of interferometric (volume) coherence to forest height. From the simulation, we obtained lower/upper boundaries of the vertical wavenumber for each forest height resulting in a successful inversion performance. In addition, the simulation results show that at least three InSAR acquisitions with various vertical wavenumbers (κ_z: <0.06, ~0.15, and >0.30 rad/m) are required in order to successfully perform the

forest height inversion from InSAR data for a wide forest height range from 3 to 60 m.

We proposed to use *a priori* knowledge of forest height to determine lower and upper boundaries of κ_z. Although the initial height information was at a lower resolution and was of a relatively poor vertical accuracy, it contributed to the selection of vertical wavenumber(s) among multiple InSAR acquisitions. In this study, mangrove height estimated from SRTM allowed us to define the lower and upper boundaries of the vertical wavenumber over the Akanda and Pongara National Parks. Globally available DEMs (e.g., TDX and ASTER) are an alternative for initial information of mangrove heights. Single-baseline inversion results within reliable κ_z ranges were selected and combined for an accurate forest height estimate. Large-scale mangrove top canopy height estimates were successfully demonstrated with the correlation coefficient of 0.98 and an RMSE of 2.73 m.

For the proposed method, *a priori* knowledge of forest height is essential to determine the κ_z ranges for a good height inversion. Up to now, only for mangrove forests, initial height information derived from global DEMs is globally available. Upcoming Global Ecosystem Dynamics Investigation (GEDI) mission [41], [42] will provide gridded height information for all forested areas between 50° north and south latitude (GEDI Level 4 product) that will serve as *a priori* height information for the proposed multibaseline height inversion approach.

REFERENCES

[1] J. S. Huxley, *Problems of Relative Growth*. New York, NY, USA: McVeagh, 1932.

[2] P. Burschel and J. Huss, *Grundriss des Waldsbaus*. Berlin, Germany: Springer-Verlag, 1997.

[3] T. Mette, K. Papathanassiou, and I. Hajnsek, "Biomass estimation from polarimetric SAR Interferometry over heterogeneous forest terrain," in *Proc. IEEE Int. Geosci. Remote Sens. Symp.*, Anchorage, AK, USA, Sep. 2004, pp. 511–514.

[4] S. R. Cloude and K. P. Papathanassiou, "Polarimetric SAR interferometry," *IEEE Trans. Geosci. Remote Sens.*, vol. 36, no. 5, pp. 1551–1565, Sep. 1998.

[5] K. P. Papathanassiou and S. R. Cloude, "Single baseline polarimetric SAR interferometry," *IEEE Trans. Geosci. Remote Sens.*, vol. 39, no. 11, pp. 2352–2363, Nov. 2001.

[6] S. R. Cloude and K. P. Papathanassiou, "Three-stage inversion process for polarimetric SAR interferometry," *Proc. Inst. Elect. Eng.—Radar Sonar Navig.*, vol. 150, no. 3, pp. 125–134, Jun. 2003.

[7] M. Neumann, S. S. Saatchi, L. M. H. Ulander, and J. E. S. Fransson, "Assessing performance of L- and P-band polarimetric interferometric SAR data in estimating boreal forest above-ground biomass," *IEEE Trans. Geosci. Remote Sens.*, vol. 50, no. 3, pp. 714–726, Mar. 2012.

[8] S. R. Cloude, "Polarization coherence tomography," *Radio Sci.*, vol. 41, no. 4, pp. 1–27, Aug. 2006.

[9] I. Hajnsek, F. Kugler, S.-K. Lee, and K. P. Papathanassiou, "Tropical-forest-parameter estimation by means of Pol-InSAR: The INDREX II campaign," *IEEE Trans. Geosci. Remote Sens.*, vol. 47, no. 2, pp. 481–493, Feb. 2009.

[10] S.-K. Lee, F. Kugler, K. P. Papathanassiou, and I. Hajnsek, "Quantification of temporal decorrelation effects at L-band for polarimetric SAR interferometry applications," *IEEE J. Sel. Topics Appl. Earth Observ. Remote Sens.*, vol. 6, no. 3, pp. 1351–1367, Jun. 2012.

[11] M. Lavalle, M. Simard, and S. Hensley, "A temporal decorrelation model for polarimetric radar interferometry," *IEEE trans. Geosci. Remote Sens.*, vol. 50, no. 7, pp. 2880–2888, Jul. 2012.

[12] M. Simard and M. Denbina, "An assessment of temporal decorrelation compensation methods for forest canopy height estimation using airborne L-band same-day repeat-pass polarimetric SAR interferometry," *IEEE J. Sel. Topics Appl. Earth Observ. Remote Sens.*, vol. 11, no. 1, pp. 95–111, Jan. 2018.

[13] F. Kugler, F. N. Koudogbo, K. P. Papathanassiou, and K. Gutjahr, "Frequency effects in POL-InSAR forest height estimation," in *Proc. Eur. Conf. Synthetic Aperture Radar*, Dresden, Germany, May 16–18, 2006, pp. 1–4.

[14] J. Praks, F. Kugler, K. P. Papathanassiou, I. Hajnsek, and M. Hallikanien, "Tree height estimation for boreal forest by means of L and X band PolInSAR and HUTSCAT profiling scatterometer," *IEEE Geosci. Remote Sens. Lett.*, vol. 4, no. 3, pp. 466–470, Jul. 2007.

[15] Y. Sadeghi, B. St-Onge, B. Leblon, and M. Simard, "Canopy height model (CHM) derived from a TanDEM-X InSAR DSM and an airborne lidar DTM in boreal forest," *IEEE J. Sel. Topics Appl. Earth Observ. Remote Sens.*, vol. 9, no. 1, pp. 381–397, Jan. 2016.

[16] M. J. Soja, J. I. H. Askne, and L. M. H. Ulander, "Estimation of boreal forest properties from TanDEM-X data using inversion of the interferometric water cloud model," *IEEE Geosci. Remote Sens. Lett.*, vol. 14, no. 7, pp. 997–1001, Jul. 2017.

[17] M. J. Soja, H. J. Persson, and L. M. H. Ulander, "Estimation of forest biomass from two-level model inversion of single-pass InSAR data," *IEEE Geosci. Remote Sens. Lett.*, vol. 53, no. 9, pp. 5083–5099, Sep. 2015.

[18] R. Treuhaft *et al.*, "Tropical-forest biomass estimation at X-band from the spaceborne TanDEM-X interferometer," *IEEE Geosci. Remote Sens. Lett.*, vol. 12, no. 2, pp. 239–243, Feb. 2015.

[19] R. Bamler and P. Hartl, "Synthetic aperture radar interferometry," *Inverse Probl.*, vol. 14, no. 4, pp. R1–R54, Aug. 1998.

[20] H. Zebker and J. Villasenor, "Decorrelation in interferometric radar echoes," *IEEE Trans. Geosci. Remote Sens.*, vol. 45, no. 10, pp. 950–959, Sep. 1992.

[21] F. Kugler, S. Sauer, S.-K. Lee, K. Papathanassiou, and I. Hajnsek, "Potential of TanDEM-X for forest parameter estimation," in *Proc. Eur. Conf. Synthetic Aperture Radar*, Aachen, Germany, 2010, pp. 1–4.

[22] F. Kugler, I. Hajnsek, D. Schulze, H. Pretzsch, and K. Papathanassiou, "TanDEM-X Pol-InSAR performance for forest height estimation," *IEEE Trans. Geosci. Remote Sens.*, vol. 52, no. 10, pp. 6404–6422, Apr. 2014.

[23] S.-K. Lee and T. E. Fatoyinbo, "TanDEM-X Pol-InSAR inversion for mangrove canopy height estimation," *IEEE J. Sel. Topics Appl. Earth Observ. Remote Sens.*, vol. 8, no. 7, pp. 3608–3618, Jul. 2015.

[24] J. M. Lopez-Sanchez, F. Vicente-Guijalba, E. Erten, M. Campos-Taberner, and F. J. Garcia-Haro, "Retrieval of vegetation height in rice fields using polarimetric SAR interferometry with TanDEM-X data," *Remote Sens. Environ.*, vol. 192, pp. 30–44, Apr. 2017.

[25] S.-K. Lee, F. Kugler, K. Papathanassiou, and I. Hajnsek, "Multibaseline polarimetric SAR interferometry forest height inversion approaches," in *Proc. 5th Int. Workshop POLinSAR*, Frascati, Italy, Jan. 24–28, 2011, pp. 1–7.

[26] F. Kugler, S.-K. Lee, I. Hajnsek, and K. Papathanassiou, "Forest height estimation by means of Pol-InSAR data inversion: The role of the vertical wavenumber," *IEEE Trans. Geosci. Remote Sens.* vol. 53, no. 10, pp. 5294–5311, Oct. 2015.

[27] M. Lavalle and K. Khun, "Three-baseline InSAR estimation of forest height," *IEEE Geosci. Remote Sens. Lett.*, vol. 11, no. 10, pp. 1737–1741, Oct. 2014.

[28] S. R. Cloude, *Polarisation: Applications in Remote Sensing*. London, U.K.: Oxford Univ. Press, 2010.

[29] R. N. Treuhaft, S. N. Madsen, M. Moghaddam, and J. J. van Zyl, "Vegetation characteristics and underlying topography from interferometric radar," *Radio Sci.*, vol. 31, no. 6, pp. 1449–1495, 1996.

[30] G. Krieger *et al.*, "TanDEM-X: A satellite formation for high-resolution SAR interferometry," *IEEE Trans. Geosci. Remote Sens.* vol. 45, no. 11, pp. 3317–3341, Nov. 2007.

[31] M. Simard *et al.*, "Mapping height and biomass of mangrove forests in Everglades National Park with SRTM elevation data," *Photogramm. Eng. Remote Sens.*, vol. 723, pp. 299–311, 2006.

[32] M. Simard, V. H. Rivera-Monroy, J. E. Mancera-Pineda, E. Castaneda-Moya, and R. R. Twilley, "A systematic method for 3D mapping of mangrove forests based on shuttle radar topography mission elevation data, ICESat/GLAS waveforms and field data: Application to Cienaga Grande de Santa Marta, Colombia," *Remote Sens. Environ.*, vol. 112, pp. 2131–2144, 2008.

[33] T. E. Fatoyinbo and M. Simard, "Height and biomass of mangroves in Africa from ICESat/GLAS and SRTM," *Int. J. Remote Sens.*, vol. 34, no. 2 pp. 668–681, Jan. 2013.

[34] T. E. Fatoyinbo, M. Simard, R. A. Washing-Allen, and H. H. Shugart, "Landscape-scale extent, height, biomass, and carbon estimation of Mozambique's mangrove forests with landsat ETM+ and shuttle radar

This article has been accepted for inclusion in a future issue of this journal. Content is final as presented, with the exception of pagination.

LEE *et al.*: MULTIBASELINE TANDEM-X MANGROVE HEIGHT ESTIMATION: THE SELECTION OF THE VERTICAL WAVENUMBER 9

topography mission elevation data," *J. Geophys. Res.*, vol. 113, 2008, Art. no. G02S06.

[35] R. F. Hanssen, *Radar Interferometry: Data Interpretation and Error Analysis*. Dordrecht, The Netherlands: Kluwer, 2001.

[36] M. Zink *et al.*, "TanDEM-X: The new global DEM takes shape," *IEEE Geosci. Remote Sens. Mag.*, vol. 2, no. 2, pp. 8–23, Jun. 2014.

[37] E. Corcoran, C. Ravilious, and M. Skuja, *Mangroves of Western and Central Africa (UNEP Biodiversity 26)*. Cambridge, MA, USA: UNEP-WCMC, 2007, (ISBN: 978-92-807-2792-0).

[38] "TanDEM-X payload ground segment: CoSSC generation and interferometric consideration," TP-PGS-TN-3129, 2012. [Online]. Available: https://tandemx-science.dlr.de/

[39] R. Z. Schneider, K. Papathanassiou, I. Hajnsek, and A. Moreira, "Polarimetric and interferometric characterization of coherent scatterers in urban areas," *IEEE Trans. Geosci. Remote Sens.*, vol. 44, no. 4, pp. 971–984, Apr. 2006.

[40] "Radiometric calibration of TerraSAR-X data: Beta naught and sigma naught coefficient calculation," INFOTERRA, Friedrichshafen, Germany, 2008.

[41] R. Dubayah *et al.*, "The global ecosystem dynamics investigation (GEDI)," in *Proc. Amer. Geophys. Union Fall Meeting*, San Francisco, CA, USA, 2014, pp. 253–266.

[42] W. Qi and R. O. Dubayah, "Combining TanDEM-X InSAR and simulated GEDI lidar observations for forest structure mapping," *Remote Sens. Environ.*, vol. 187, pp. 253–266, Dec. 2016.

[43] T. Fatoyinbo, E. Feliciano, D. Lagomasino, S.-K. Lee, and C. Trettin, "Estimating mangrove aboveground biomass from airborne Lidar data: A case study from the Zambezi river delta," *Environ. Res. Lett.*, vol. 13, pp. 1–13, Feb. 2018.

David Lagomasino received the Ph.D. degree in geological sciences from Florida International University, Miami, FL, USA, in 2014. He is currently a remote Sensing Scientist with a strong background in coastal hydrogeology.

His research interests include land-water-atmosphere interactions, coastal ecosystem services, mangrove wetlands, and more specifically, land use change, forest and wetland cover and structure modeling, and water–carbon cycle science at the land–sea interface.

Emanuelle Feliciano received the B.S. degree in geology from the University of Puerto Rico, Mayaguez Campus, Mayaguez, Puerto Rico, in 2009, and the Ph.D. degree in marine geology and geophysics from the Rosenstiel School of Marine and Atmospheric Science, University of Miami, Miami, FL, USA, in 2015.

Since 2015, he has been a Postdoctoral Fellow with the Biospheric Sciences Laboratory, NASA Goddard Space Flight Center, Greenbelt, MD, USA. His research interests include the characterization and estimation of wetland forest structure, carbon and biomass using ground based and airborne Lidar, and EO sensors.

Seung-Kuk Lee received the B.S. and M.S. degrees in geology from Yonsei University, Seoul, South Korea, in 2000 and 2005, respectively, and the Ph.D. degree in environmental engineering from ETH Zurich, Zurich, Switzerland, in 2013.

From 2006 to 2013, he was with the Microwaves and Radar Institute (HR), German Aerospace Center (DLR), Oberpfaffenhofen, Germany. In 2013, he started to work with the Biospheric Sciences Laboratory , NASA Goddard Space Flight Center (GSFC), USA. From 2014 to 2016, he was a NASA Postdoctoral Fellow with NASA/GSFC. He is currently a Scientist with the NASA/GSFC, Greenbelt, MD, USA, and an Assistant Research Professor with the University of Maryland, College Park, MD, USA. His research interests include 3-D forest parameter estimation using polarimetry SAR interferometry techniques and analysis of SAR images for terrestrial ecosystem applications.

Dr. Lee is a science definition team member of the Global Ecosystem Dynamics Investigation mission for the fusion of spaceborne Lidar and InSAR data.

Carl Trettin received the B.S. degree in forest hydrology and M.S. degree in forest soils from Michigan Technological University, Houghton, MI, USA, in 1976 and 1980, respectively, and the Ph.D. degree in forest soils from North Carolina State University in 1992.

He was a Research Scientist with Michigan Technological University, from 1978 to 1988, and with Oak Ridge National Laboratory, Oak Ridge, TN, USA, from 1991 to 1994. Since 1994, he has been a Research Scientist and a Team Leader with the USDA Forest Service, Southern Research Station, Asheville, NC, USA. His work in African mangroves considers the quantification of carbon stocks in biomass and soils, which led to collaborations for the application of remote sensing data for assessing these remote but important ecosystems. His research focuses on carbon biogeochemistry in forested wetlands ranging from the tropics to the boreal zone.

Temilola (Lola) E. Fatoyinbo received the Ph.D. degree in environmental sciences from the University of Virginia, Charlottesville, VA, USA, in 2008.

From 2008 to 2009, she was a Postdoctoral Candidate with the Radar Remote Sensing Group, California Institute of Technology/NASA Jet Propulsion Laboratory, Pasadena, CA, USA.

Since 2010, she has been a Research Scientist in Earth Science Remote Sensing with the Biospheric Sciences Laboratory, Goddard Space Flight Center, Greenbelt, MD, USA. She also works on new instrument technology development and serves as the PI for the EcoSAR instrument and member of the Global Ecosystem Dynamics Investigation science team. Her research interests include the use of passive optical, SAR and Lidar data for forest structure, biomass and carbon estimation in coastal and terrestrial tropical systems, and using remote sensing for conservation and ecosystem service accounting.

Dr. Fatoyinbo is the recipient of the 2011 Presidential Early Career Award for Scientists and Engineers.